Supporting information for

A Translocation Fluorescent Probe for Analyzing Cellular Physiology Parameters in Neurological Disease Models

Zi-Lu Li,[a] Ai-Xin Ma,[a] Jing-Qi Liu,[a] Kun Wang,[b] Bao-Cun Zhu,[b,*] Dai-Wen Pang,[a,*] De-Ming Kong[a,c*]

[a]State Key Labatory of Medicinal Chemical Biology, Tianjin Key Laboratory of Biosensing and Molecular Recognition, Research Centre for Analytical Sciences, College of Chemistry, Nankai University, Tianjin, 300071, P. R. China.

[b]School of Water Conservancy and Environment, University of Jinan, Jinan, 250022, P. R. China.

[c]School of Chemistry and Chemical Engineering, Qinghai Minzu University, Xining 810007, Qinghai Province, P. R. China.

Table of Contents

22. **OQ** fluorescence images of PC12 cells treated with MPP^+ and melatonin for different time

23. **OQ** fluorescence images of PC12 cells without JEV infection

24. Rhodamine 123 fluorescence images of JEV-infected cells

25. JC-1 fluorescence images of JEV-infected cells

1. Materials and methods

The Hoechst, Mito-Tracker, Rhodamine 123, and JC-1 (5,5,6,6-tetrachloro-1,1,3,3-tetraethylbenzimidazolylcarbocyanine iodide), were purchased from Shanghai Macklin Biochemical Technology Co. Ltd. Melatonin and 1-Methyl-4-phenylpyridinium iodide (MPP^+) were purchased from Beijing Solarbio Science & Technology Co. Ltd.

The fluorescence spectra were recorded on the Shimadzu RF-5301 PC fluorescence spectrometer, manufactured by Shimadzu Ltd. in Japan. Ultraviolet-visible (UV-Vis) spectra were recorded on the TU-1901 spectrophotometer (Persee, Beijing). For photographing the fluorescence images of cells, a confocal laser scanning microscope (CLSM) setup was utilized. The specific model used was the Nikon A^+, which was equipped with a 60 × oil objective lens. ^{1}H-nuclear magnetic resonance (NMR) data were obtained by Bruker AV-400 NMR spectrometer. ^{13}C-NMR data were obtained by Bruker AV-600 NMR spectrometer. High resolution mass spectrometry (HRMS) data were obtained by Agilent 21905990.

2. Synthesis of PQ and OQ

OQ and **PQ** were synthesized according to the procedures shown in **Scheme S1**.

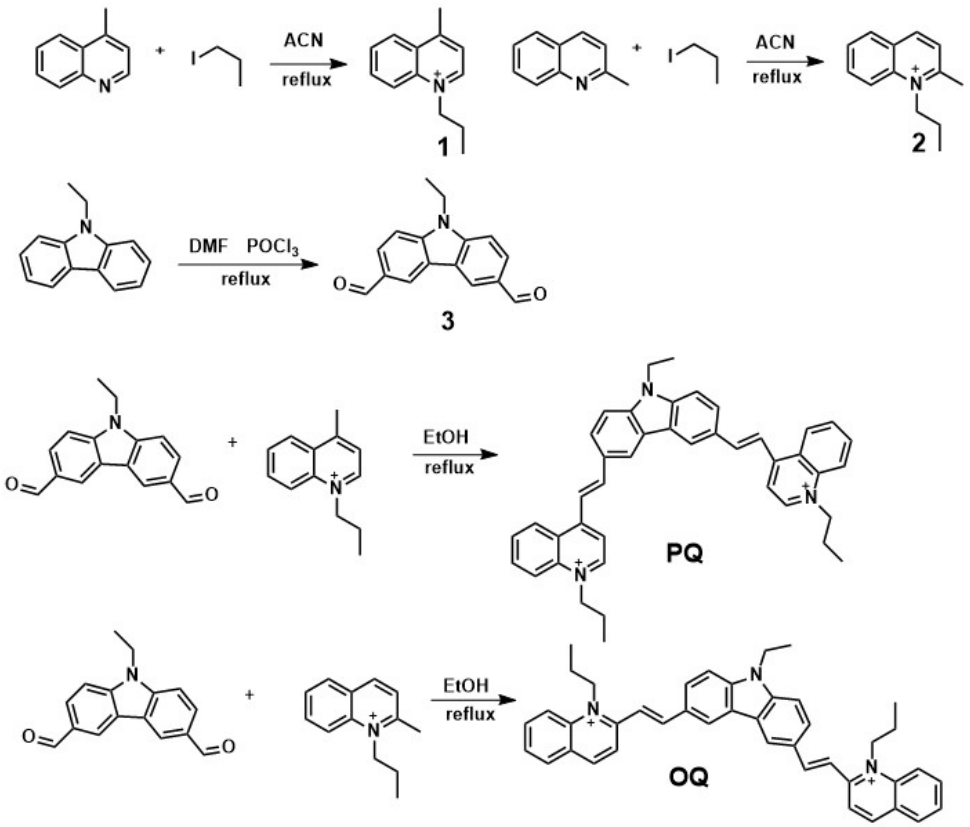

Scheme S1. Synthetic scheme of **OQ** and **PQ**.

Synthesis of compounds **1** and **2**

2-methylquinoline (0.286 g, 2 mmol) dissolve in 20 mL of acetonitrile, add iodopropane (1.5 g, 10 mol). The reaction was go in sealed pressure tube at 80°C for 12h. the reaction solution removed solvent by vacuum rotary steam, and then purified by silica gel column chromatography (dichloromethane: methanol = 40:1, v/v) to obtain solid compound 1 was 0.445 g, yield 25%. ^{1}H NMR (400 MHz, DMSO-d_6) δ 9.42 (d, J = 6.0 Hz, 1H), 8.71 – 8.49 (m, 2H), 8.35 – 8.18 (m, 1H), 8.15 – 7.99 (m, 2H), 4.98 (t, J = 7.4 Hz, 2H), 3.01 (s, 3H), 1.98 (q, J = 7.4 Hz, 2H), 0.96 (t, J = 7.3 Hz, 3H).

4-methylquinoline (0.286 g, 2 mmol) dissolve in 20 mL of acetonitrile, add iodopropane (1.5 g, 10 mol). The reaction was go in sealed pressure tube at 80°C for 12h. the reaction solution removed solvent by vacuum rotary steam, and then purified by silica gel column chromatography (dichloromethane: methanol = 40:1, v/v) to obtain solid compound 1 was 0.535 g, yield 30%. ^{1}H NMR (400 MHz, DMSO-d_6) δ 9.11 (d, J = 8.5 Hz, 1H), 8.62 (d, J = 9.0 Hz, 1H), 8.42 (m, J = 8.0, 1.6 Hz, 1H), 8.23 (t, J = 8.9, 7.0, 1.6 Hz, 1H), 8.14 (d, J = 8.5 Hz, 1H), 8.00 (t, J = 7.5 Hz, 1H), 5.01 – 4.78 (m, 2H), 3.12 (s, 3H), 1.92 (q, J = 7.8 Hz, 2H), 1.12 (t, J = 7.3 Hz, 3H).

Synthesis of Compound **3**

Compound **3** were synthesized as reported in the literature 1.

Reference

1. Xu, W.; Ma, P.; Diao, Q.; Xu, L.; Liu, X.; Sun, Y.; Wang, X.; Song, D. *Sens. Actuators B Chem.* **2017**, *252*, 86–94.

Synthesis of **OQ**

Compounds **3** (0.5 mmol, 0.125 g) and **2** (1 mmol, 0.186 g) were dissolved in 20 mL of EtOH, and a small amount of piperazine was added. The obtained mixture was refluxed for 12 h, cooled to room temperature and then purified on a silica gel column (DCM:MeOH=50:1) to give a red solid (0.080 g) in 25% yield. ^{1}H-NMR (400 MHz, DMSO-d_6) δ 9.10-8.90 (m, 4H), 8.67 (d, J = 9.0 Hz, 2H), 8.59-8.48 (m, 4H), 8.33 (d, J = 8.0 Hz, 2H), 8.25-8.08 (m, 4H), 8.03 -7.81 (m, 6H), 5.16 (t, J = 7.9 Hz, 4H), 4.56 (d, J = 7.4 Hz, 2H), 2.04 -1.95 (m, 4H), 1.38 (t, J=6.6 Hz, 3H), 1.17 (m, 6H). ^{13}C-NMR (101 MHz, DMSO-d_6) δ 155.76, 149.23, 143.72, 142.30, 138.33, 134.96, 130.35,

128.81, 128.41, 127.85, 127.15, 123.17, 122.90, 121.02, 119.08, 115.61, 110.74, 22.27, 13.96, 10.83. HRMS (m/z): $[M-2I]^{2+}$ calcd for 293.665; Found, 293.6649.

Synthesis of **PQ**

Compounds **3** (0.5 mmol, 0.125 g) and **1** (1 mmol, 0.186 g) were dissolved in 20 mL of EtOH, and a small amount of piperazine was added. Then, the mixture was refluxed for 12 h, cooled to room temperature and purified by silica gel column (DCM:MeOH=50:1) to give red solid (0.075 g) in 24% yield. ^{1}H-NMR (400 MHz, DMSO-d_6) δ 9.36 (d, J = 6.6 Hz, 2H), 9.05 (br.s, 2H), 8.55 (t, J = 6.7 Hz, 4H), 8.45 (br.s, 4H), 8.34-8.12 (m, 4H), 8.34-8.12 (m, 4H), 8.06 (t, J = 7.6 Hz, 2H), 7.85 (d, J = 8.5 Hz, 2H).4.94 (t, J = 7.1 Hz, 4H), 4.58 (d, J = 8.2 Hz, 2H), 2.06-1.94 (m, 4H), 1.42 (t, J = 7.1 Hz, 3H), 1.01 (t, J = 7.5 Hz, 6H). ^{13}C-NMR (100 MHz, DMSO-d_6) δ 153.12, 147.05, 144.67, 141.89, 137.90, 135.04, 128.97, 128.25, 127.67, 127.11, 126.57, 123.05, 122.26, 119.14, 116.99, 115.49, 110.47, 57.69, 22.82, 13.98, 10.68. HRMS (m/z): $[M-2I]^{2+}$ calcd for 293.665; Found, 293.6647.

3. Characterization of compounds

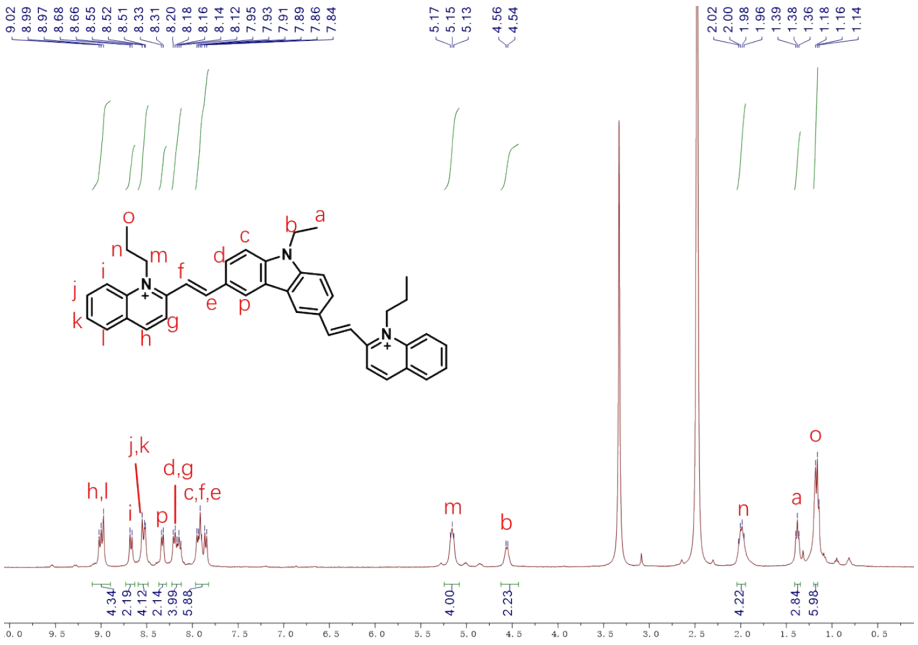

Figure S1. ^{1}H-NMR data of probe **OQ**.

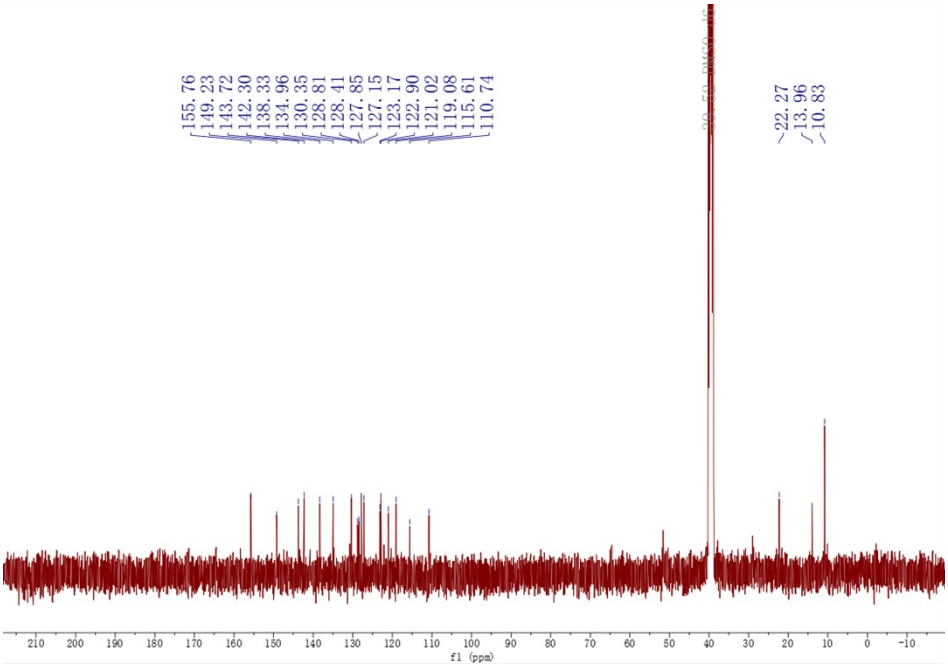

Figure S2. ^{13}C-NMR data of probe **OQ**.

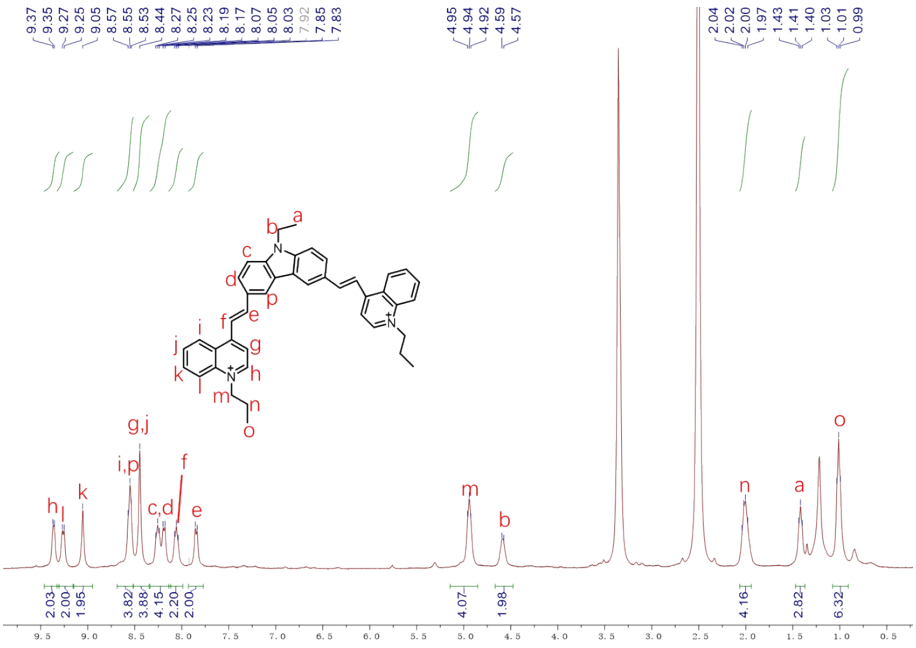

Figure S3. ^{1}H-NMR data of probe **PQ**.

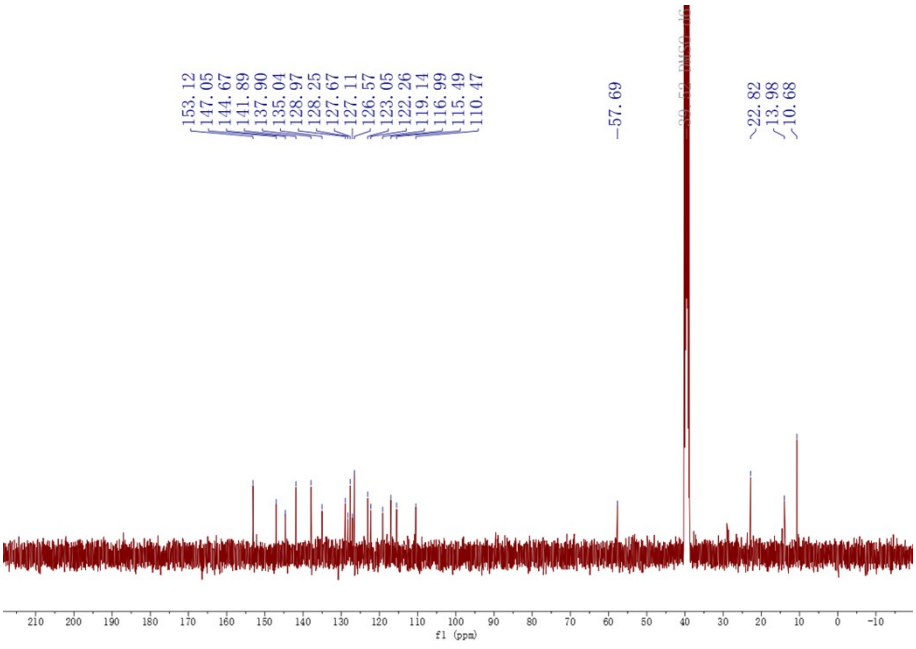

Figure S4. ^{13}C-NMR data of probe **PQ**.

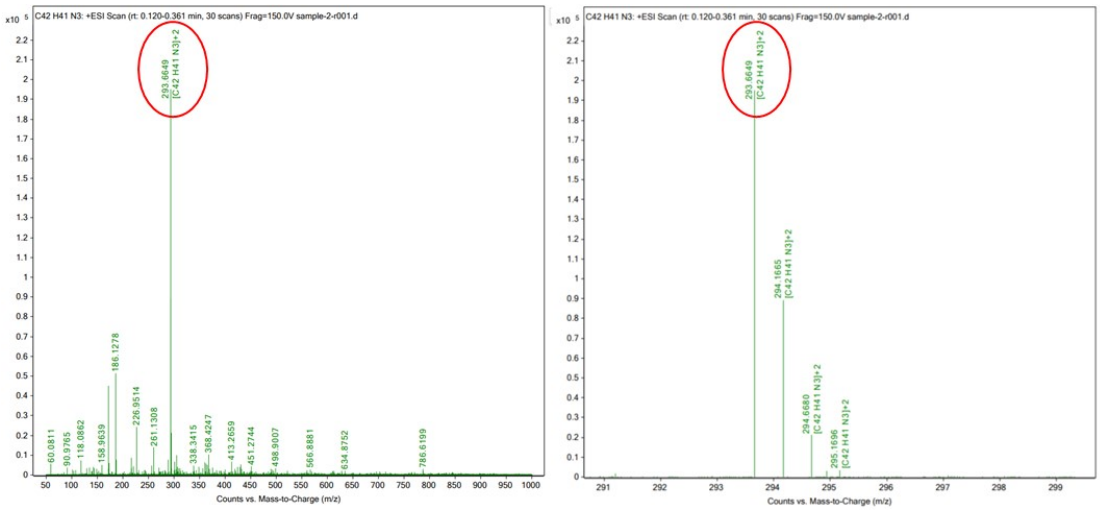

Figure S5. HRMS data of probe **OQ**.

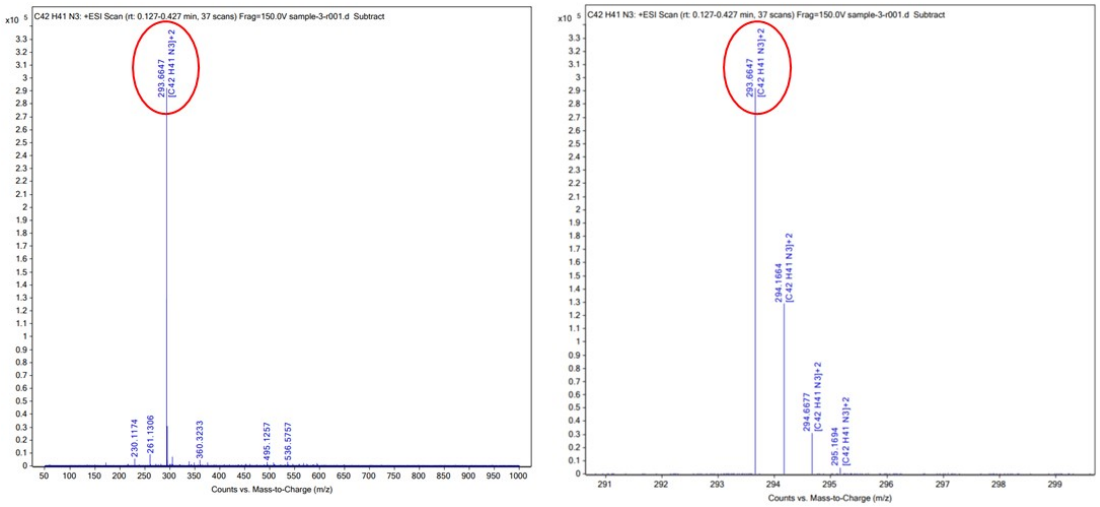

Figure S6. HRMS data of probe **PQ**.

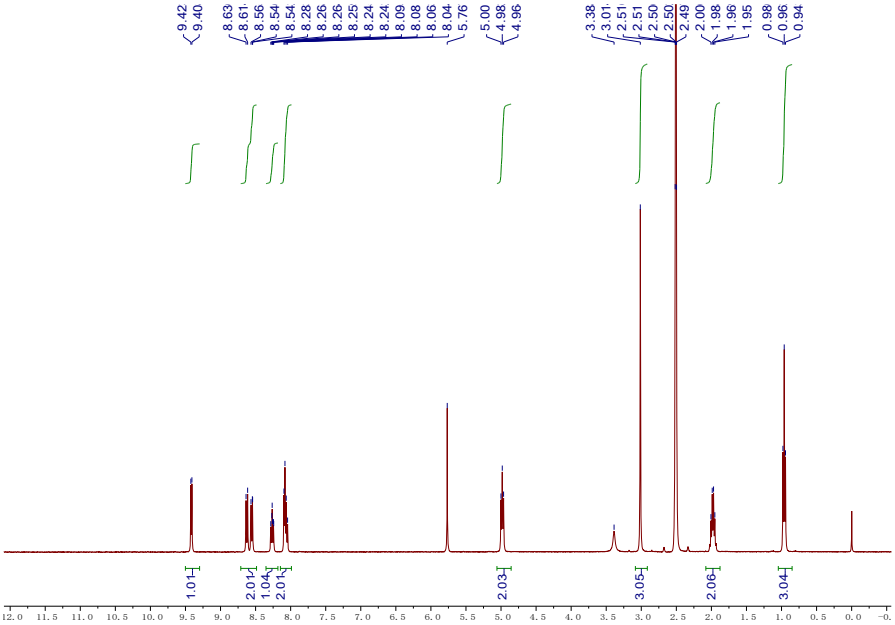

Figure S7. [1]H-NMR data of compound **1**.

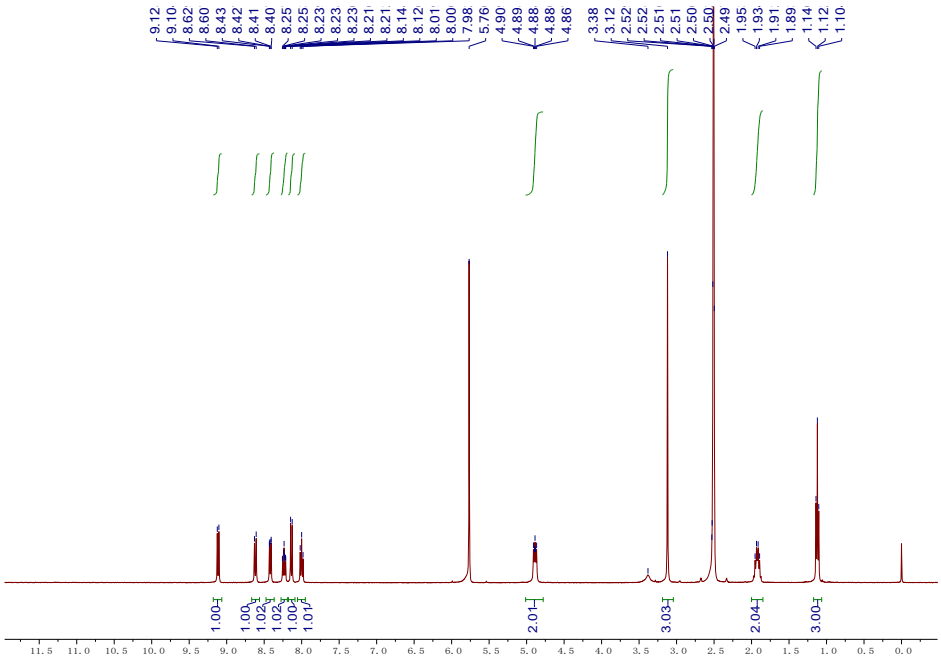

Figure S8. [1]H-NMR data of compound **2**.

4. pH-dependent fluorescence changes of OQ and PQ

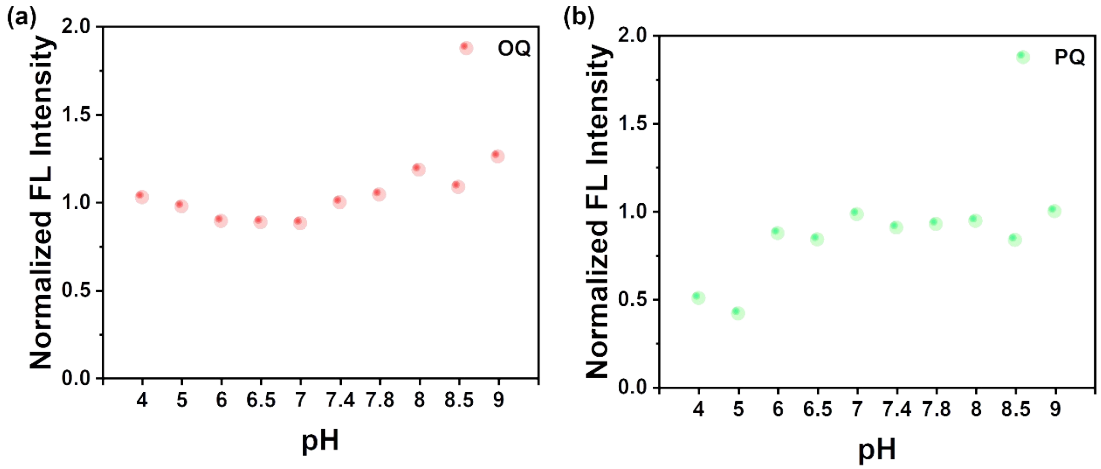

Figure S9. pH-dependent fluorescence changes of **OQ** and **PQ**. (a) λ_{ex}= 480 nm, λ_{em}= 655 nm. (b) λ_{ex}= 480 nm. λ_{em}= 700 nm.

5. Measurement of binding parameters of probe to DNA

The intrinsic constants (k) of **OQ/PQ** and DNA was acquired by the fluorescence titration method. The fluorescence intensity measured for probe was analyzed with the Scatchard equation which has been widely used in ligand-DNA binding research. The equation was displayed as the following equation (1)

$$r/C_f = k_n - k_r \quad (1)$$

Where r represents the moles of the binding dye per mole of DNA, C_f represents the molar concentration of free dye, k represents the equilibrium binding constant, n represents the number of dye sites per phosphate.

The concentration of binding probe was calculated by equation (2)

$$C_b = S_0(F-F_0)/(F_{max}-F_0) \quad (2)$$

Where S_0 is the total dye concentration, F is the fluorescence intensity of probe at the given DNA concentration, F_0 is the initial fluorescence intensity in the absence of DNA and F_{max} is the intensity of totally bound dye.

According to equation (2), r and C_f can be calculated by equations (3) and (4)

$$r = C_b/C \quad (3)$$

$$C_f = S_0 - C_b \quad (4)$$

Where C represents the given DNA concentration.

6. Molecular dynamics simulation

The molecular dynamics simulations were carried out by using GROMACS 2020.3 software. The force field parameters of the membrane and small molecules were obtained from the charmm-gui server. The simulation box size was optimized with the distance between each atom of the protein and the box greater than 1.0 nm. Then, the box was filled with water molecules based on a density of 1. To make the simulation system electrically neutral, the water molecules were replaced with Cl^- and Na^+ ions. Following the steepest descent method, energy optimization of 5.0×10^4 steps was performed to minimize the energy consumption of the entire system, and finally to reduce the unreasonable contact or atom overlap in the entire system. After energy minimization, first-phase equilibration was performed with the NVT ensemble at 300 K for 100 ps to stabilize the temperature of the system. Second-phase equilibration was simulated with the NPT ensemble at 1 bar and 100 ps. The primary objective of the simulation is to optimize the interaction between the target protein and the solvent and

ions so that the simulation system is fully pre-equilibrated. All molecular dynamics simulations were performed for 50 ns under an isothermal and isostatic ensemble with a temperature of 300 K and a pressure of 1 atmosphere. The temperature and pressure were controlled by the V-rescale and Parrinello-Rahman methods, respectively, and the temperature and pressure coupling constants were 0.1 and 0.5 ps, respectively. Lennard-Jones function was used to calculate the Van der Waals force, and the nonbond truncation distance was set to 1.4 nm. The bond length of all atoms was constrained by the LINCS algorithm. The long-range electrostatic interaction was calculated by the Particle Mesh-Ewald method with the Fourier spacing 0.16 nm.

7. Molecular docking

The initial structures of DNA were downloaded from RCSB Protein Data Bank (PDB code:43DB). The original ligand and water were removed by PyMOL for docking studies. Ligand (**OQ** and **PQ**) was prepared using the optimized compound structure. After that, the docking calculations were performed by the AutoDock 4.2 suite of programs, using ligand flexible docking approach that allows ligand flexibility. The Lamarckian genetic algorithm was chosen as the search protocol using the default parameters except for number of GA runs (ga_run = 50) and the maximum number of energy evaluations (ga_num_evals = 2500000). The displaying images were rendered with PyMOL.

8. Cytotoxicity assay

The cell viability of PC12 cells treated with probe **OQ** or **PQ** was assessed by a cell counting kit-8 (*CCK-8*; Dojindo Molecular Technologies, Tokyo, Japan). Briefly, PC12 cells, seeded at a density of 1×10^6 cells·mL^{-1} in a 96-well plate, were maintained at 37 °C in a 5% CO_2/95% air incubator for 12 h. Then the live PC12 cells were incubated with varied concentrations (0, 5, 10, 15, 20 μM) of probe **OQ** or **PQ** suspended in culture medium for 24 h. Subsequently, *CCK-8* solution was added into each well for 2 h, and the absorbance at 450 nm was measured.

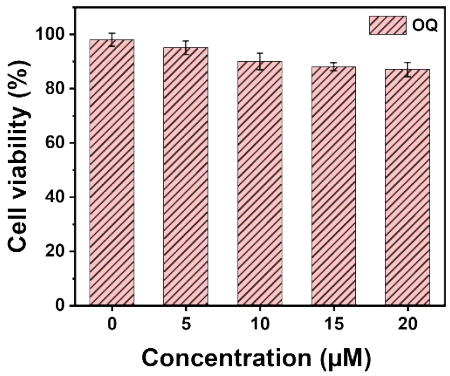

Figure S10. Cytotoxicity testing of **OQ** with a *CCK-8* assay towards PC12 cells.

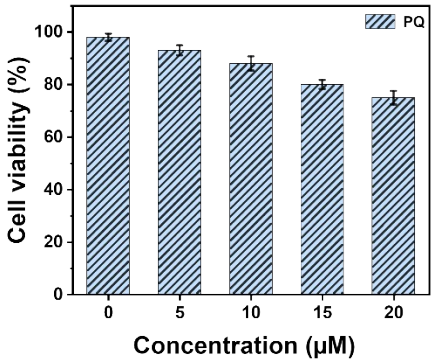

Figure S11. Cytotoxicity testing of **PQ** with a *CCK-8* assay towards PC12 cells.

9. Cell culture and staining analysis

PC12 cells were cultured in Dulbecco's modiffed Eagle medium (DMEM; Gibco) with 10% fetal bovine serum (FBS) and 1% penicillin-streptomycin, at 37 ^{o}C under a 5% CO_2 atmosphere. For live cells imaging experiments, the culture medium of cells was firstly removed, and the cells were washed with PBS buffer twice. Then, the cells were incubated in 1 mL of PBS buffer. Meanwhile, 10 mM stock solutions of the probe **OQ** and **PQ** were prepared in DMSO. After that, 1 μL of probe stock solutions were mixed evenly with 1 mL PBS buffer (pH 7.4) in a tube. The cells were incubated with the above mixed solutions at 37 ^{o}C. After incubation, the cells were imaged immediately without further washing procedure.

10. Cells and viruses

Baby hamster kidney (BHK-21) cells were maintained in Dulbecco's modiffed Eagle medium (DMEM; Gibco) containing 5% fetal bovine serum (FBS) (Gibco/Invitrogen) in an environment with 5% CO_2. The cells were discarded after 10 passages and new frozen cells were thawed. JEV SA-14-14-2 (GenBank accession number AF315119) was propagated in the BHK-21 cells and then puriffed by differential centrifugation and density gradient ultracentrifugation. The harvested viruses were eventually divided and stored at −80 °C for use.

11. OQ concentration-dependent images of PC12 cells

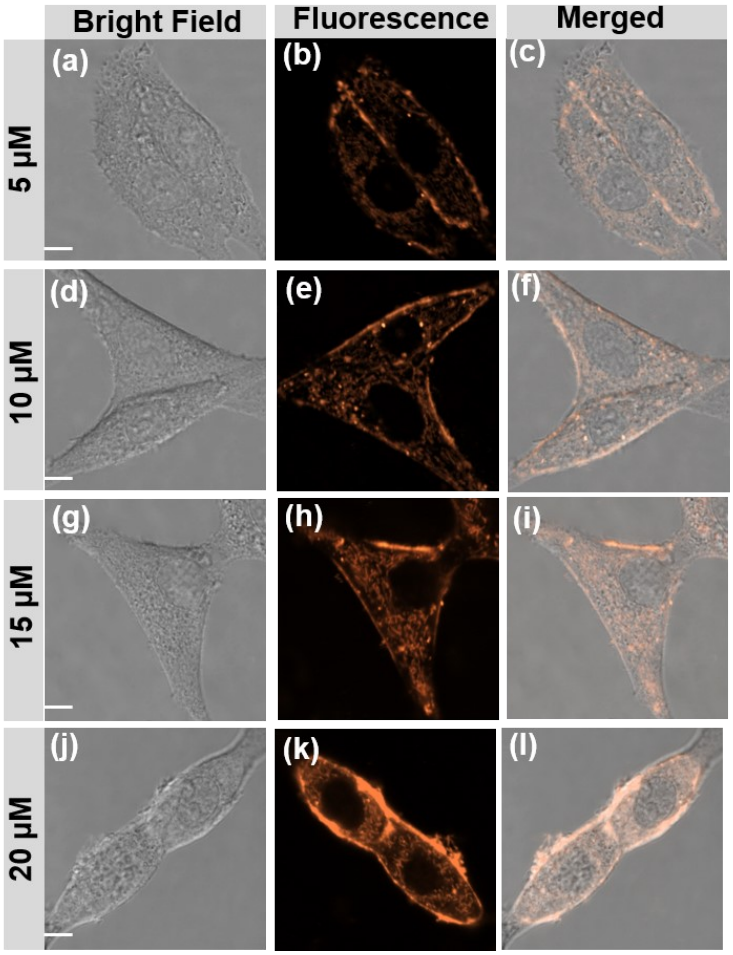

Figure S12. CLSM images of PC12 cells stained with different concentrations of **OQ**. (a-c) 5 μM, (d-f) 10 μM, (g-i) 15 μM, (j-l) 20 μM. Scale bars: 5 μm. Imaging wavelength $\lambda_{ex}/\lambda_{em}$: 560/580−650 nm.

12. PQ concentration-dependent images of PC12 cells

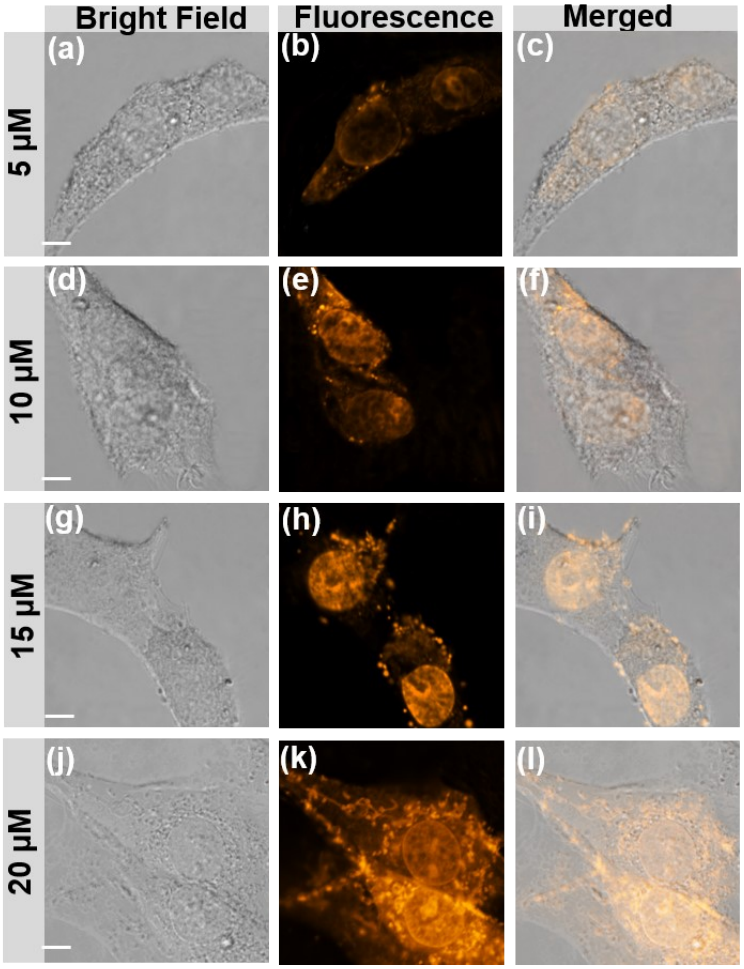

Figure S13. CLSM images of PC12 cells stained with different concentrations of **PQ**. (a-c) 5 μM, (d-f) 10 μM, (g-i) 15 μM, (j-l) 20 μM. Scale bars: 5 μm. Imaging wavelength $\lambda_{ex}/\lambda_{em}$: 560/580−650 nm.

13. Colocalization analysis of PQ and Hoechst

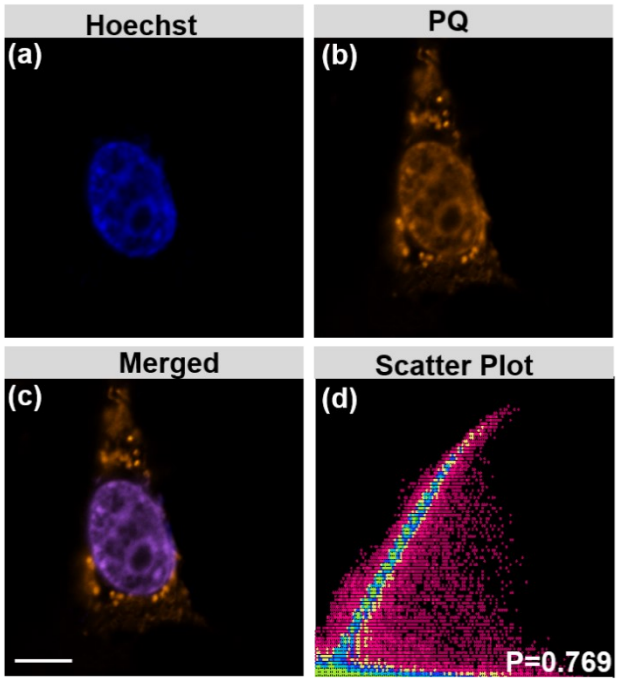

Figure S14. (a)-(c) CLSM images of PC12 cells stained with **PQ** (10 μM) and Hoechst (10 μM). (d) Pearson's co-localization coefficient of **PQ** and Hoechst. Imaging wavelength: $\lambda_{ex}/\lambda_{em}$(Hoechst): 409/410−460 nm, $\lambda_{ex}/\lambda_{em}$(**PQ**): 560/580−650 nm. Scale bars: 5 μm.

14. Colocalization analysis of PQ and Mito-Tracker green

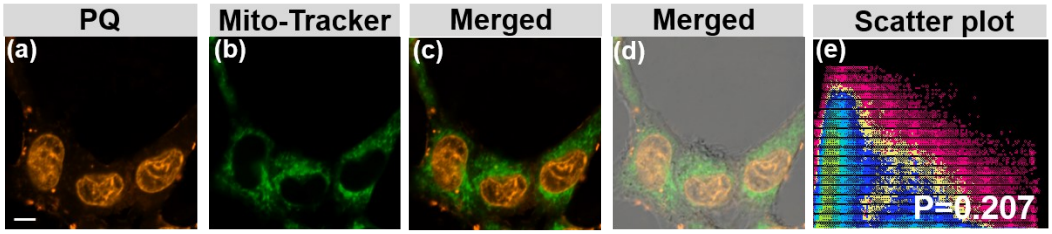

Figure S15. (a)-(d) CLSM images of PC12 cells treated with **PQ** (10 μM) and Mito-Tracker green (10 μM). (e) Pearson's co-localization coefficient of **PQ** and Mito-Tracker green. Imaging wavelength:$\lambda_{ex}/\lambda_{em}$ (Mito-Tracker) 487/500−550 nm, λex/λem (**PQ**): 560/580−650 nm. Scale bars: 5 μm.

15. Staining apoptotic PC12 cells with PQ

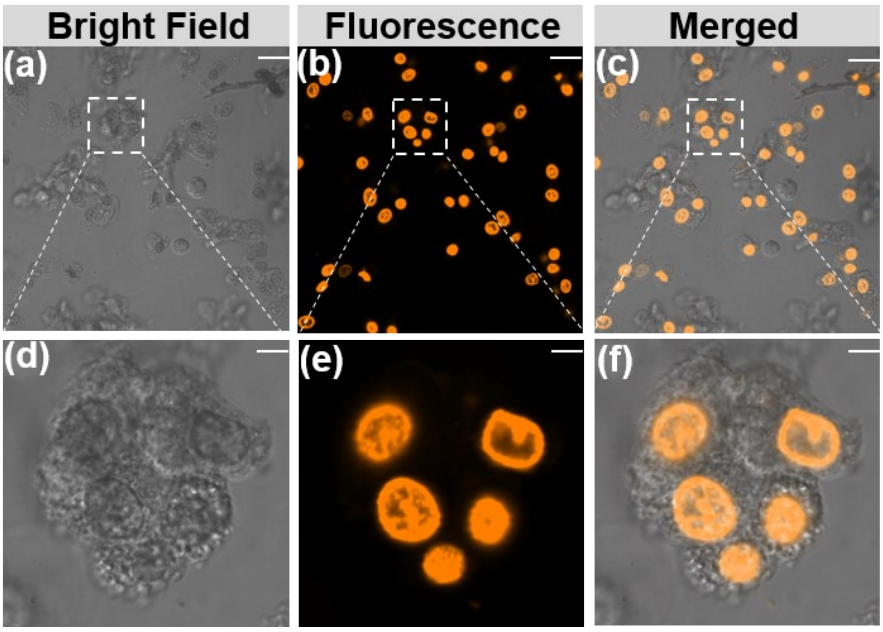

Figure S16. CLSM images of PC12 cells pretreated with cisplatin (5 μM) for 12 h and then treated with **PQ** (10 μM). Scale bars: (a)-(c) 20 μm, (d)-(f) 5 μm.

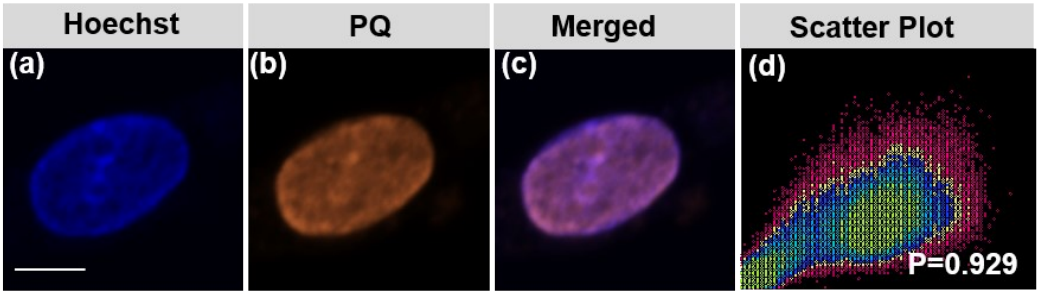

Figure S17. (a)-(c) CLSM images of PC12 cells pretreated with cisplatin (5 μM) for 12 h and then treated with **PQ** (10 μM) and Hoechst (10 μM). (d) Pearson's co-localization coefficient of **PQ** and Hoechst. Imaging wavelength: $\lambda_{ex}/\lambda_{em}$(Hoechst): 409/410−460 nm, $\lambda_{ex}/\lambda_{em}$(**PQ**): 560/580−650 nm. Scale bars: 5 μm.

16. Time-dependent total interaciton energy of OQ and PQ with DOPC layer

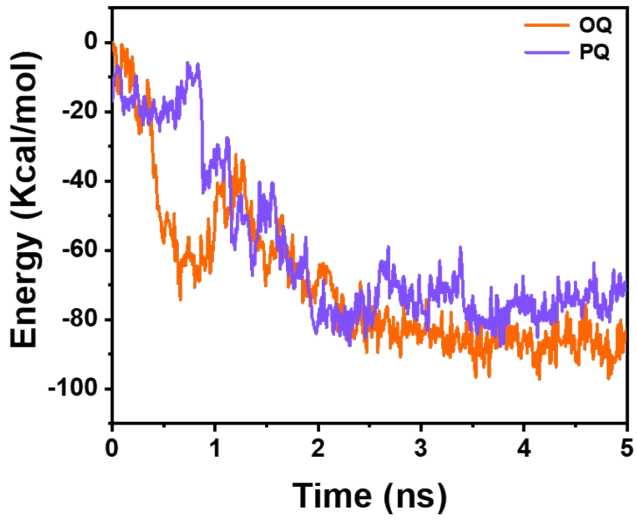

Figure S18. The total interaction energy changes of the probes with the DOPC layer over time.

17. Effects of viscosity on the fluorescence of OQ and PQ

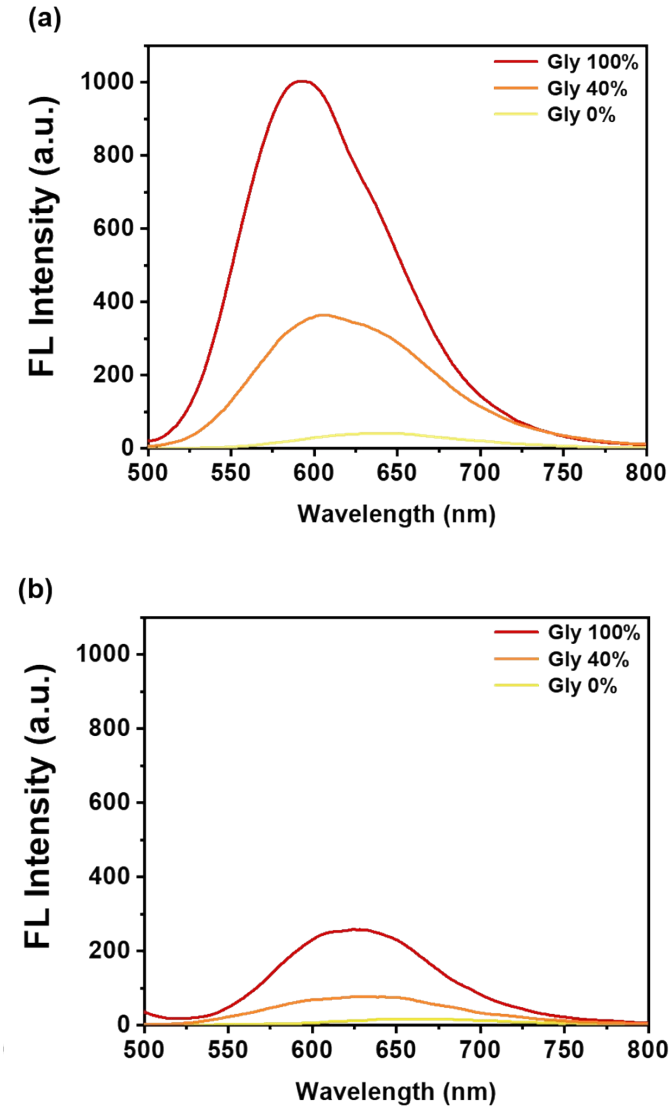

Figure S19. The emission spectra of (a) **OQ** (10 μM) and (b) **PQ** (10 μM) in methanol–Gly mixed solvents containging different Gly percentages. λ_{ex}= 480 nm. Slit widths: 1.5 nm, 3 nm.

18. Surface area of OQ and PQ in different electrostatic potential ranges

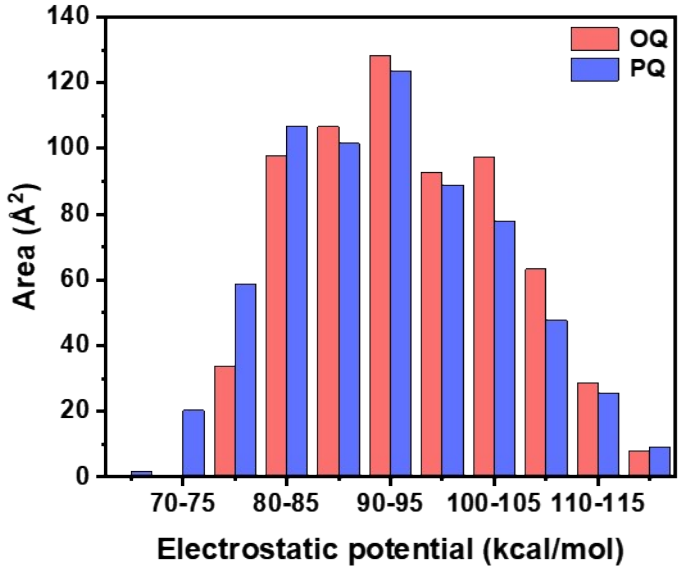

Figure S20. Surface area of **OQ** and **PQ** in different electrostatic potential ranges.

19. Oxidative stress-induced rapid changes of cell status oberved by OQ

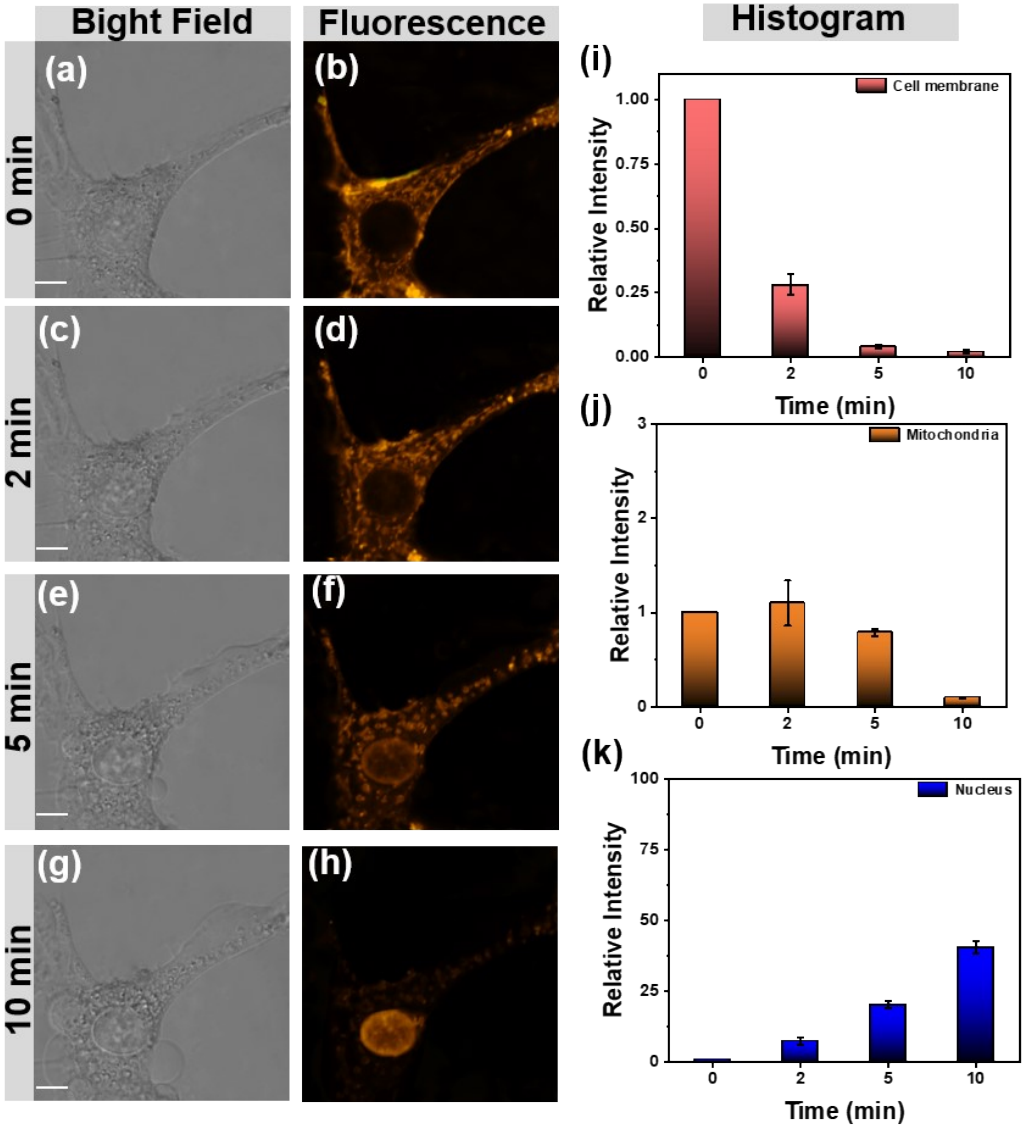

Figure S21. CLSM images of PC12 cells treated with H_2O_2 (5 mM) , followed by staining with **OQ** (10 μM). Scale bars: 5 μm.

20. OQ fluorescence images of PC12 cells treated with different concentration of MPP^+

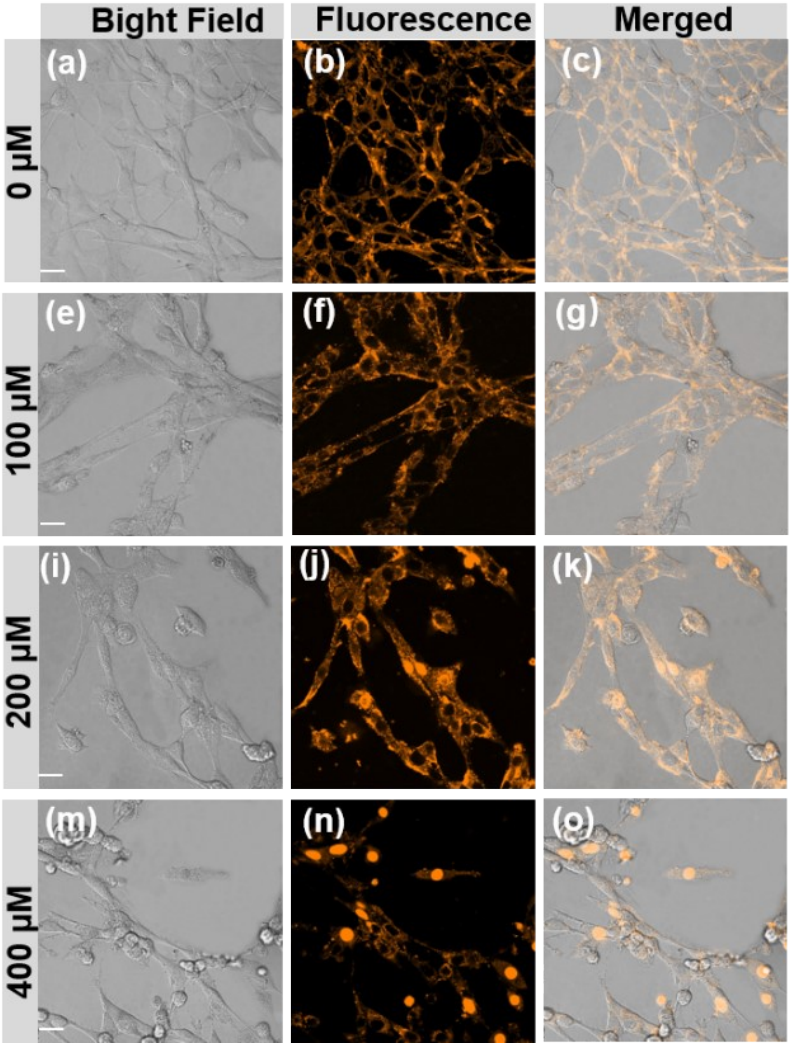

Figure S22. CLSM images of PC12 cells treated with different concentration of MPP^+ for 36 h, followed by staining with **OQ** (10 μM). Imaging wavelength $\lambda_{ex}/\lambda_{em}$: 560/580−650 nm. Scale bars: 20 μm.

21. OQ fluorescence images of PC12 cells treated with MPP^+ for different time

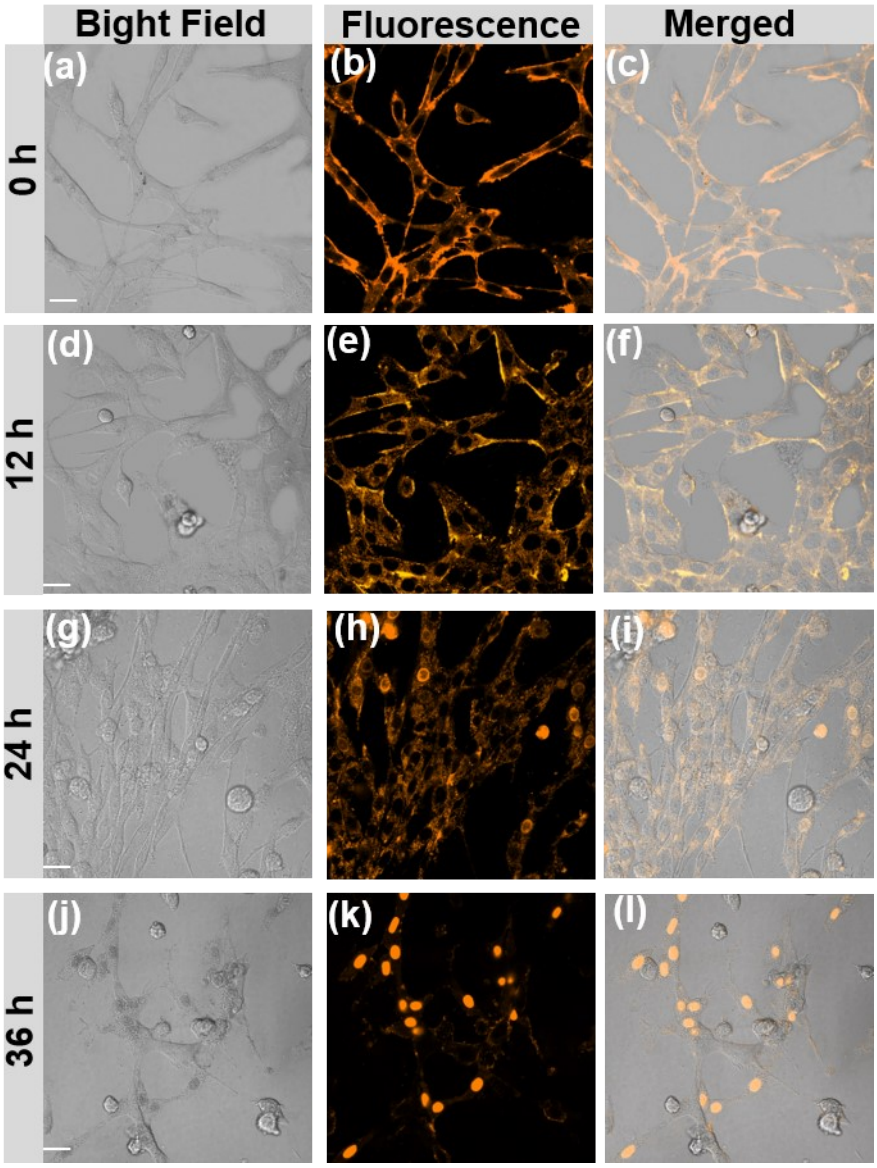

Figure S23. CLSM images of PC12 cells treated with MPP^+ (400 μM) for different time, followed by staining with **OQ** (10 μM) .Imaging wavelength $\lambda_{ex}/\lambda_{em}$: 560/580−650 nm. Scale bars: 20 μm.

22. OQ fluorescence images of PC12 cells treated with MPP^+ and melatonin for different time

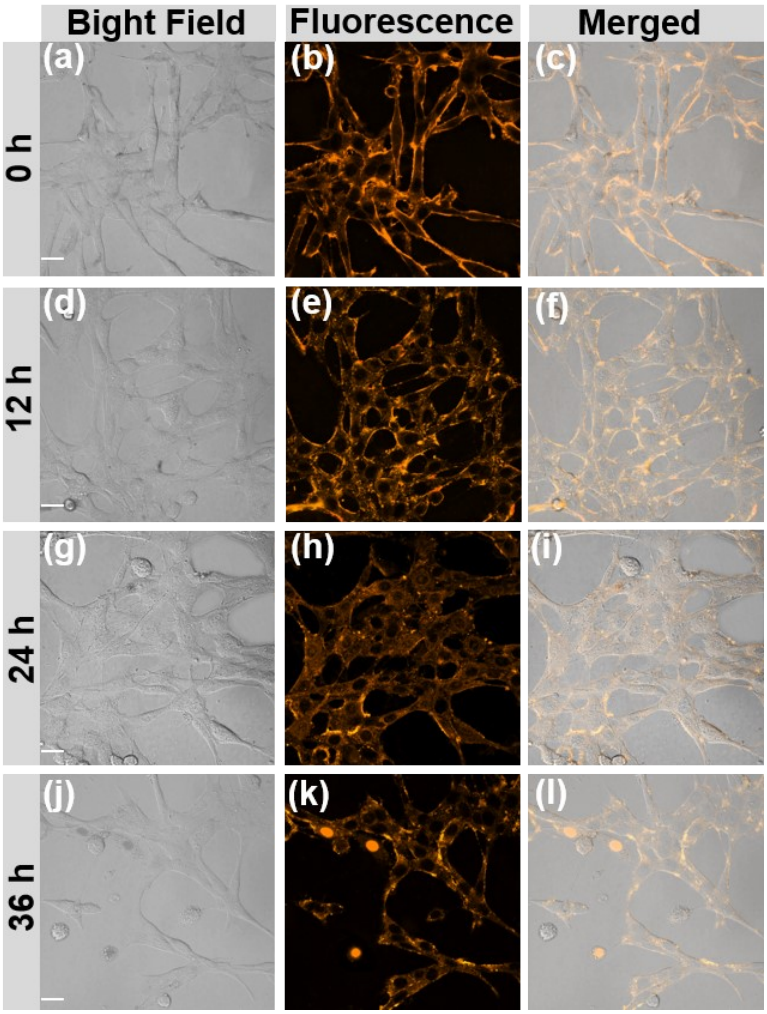

Figure S24. **OQ** fluorescence images of PC12 cells treated with MPP^+ (400 μM) and melatonin (300 μM) for different time. Melatonin was added after MPP^+ treatment for 12 h. Imaging wavelength $\lambda_{ex}/\lambda_{em}$: 560/580−650 nm. Scale bars: 20 μm.

23. OQ fluorescence images of BHK-21 cells without JEV infection

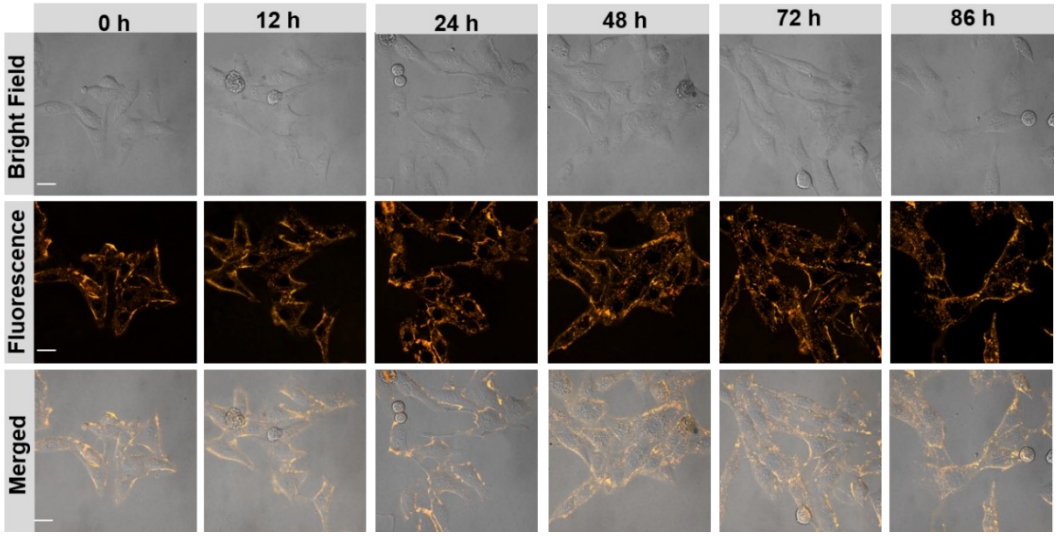

Figure S25. **OQ** fluorescence images of BHK-21 cells without JEV infection. Scale bars: 20 μm.

24. Rhodamine 123 fluorescence images of JEV-infected cells

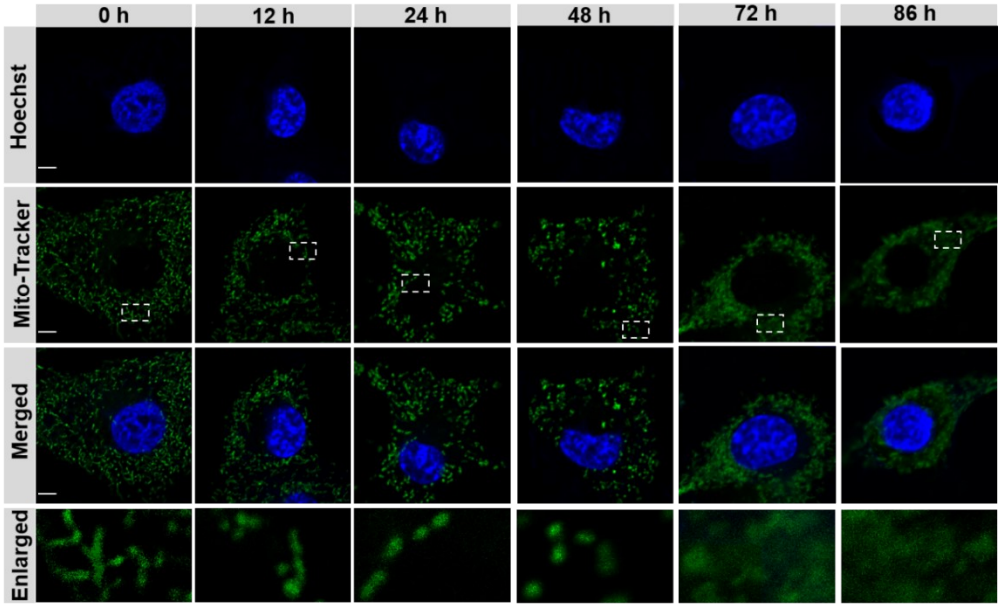

Figure S26. CLSM images of BHK-21 cells treated with JEV (MOI=0.5) for different time, followed by staining with Hoechst (10 μM) and Rhodamine 123 (5 μM). Imaging wavelength $\lambda_{ex}/\lambda_{em}$: 409/410−460 nm for Hoechst, 487/500−550 nm for Rhodamine 123. Scale bars: 5 μm.

25. JC-1 fluorescence images of JEV-infected cells

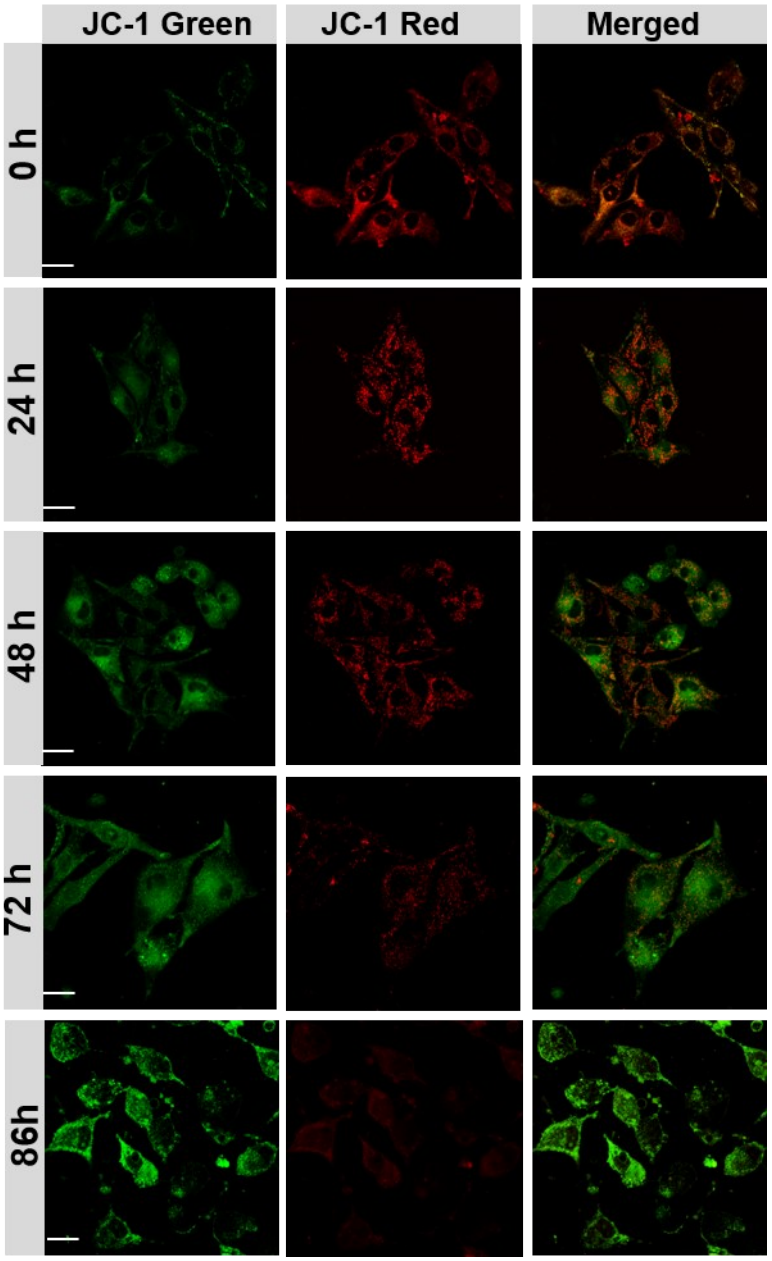

Figure S27. CLSM images of BHK-21 cells treated with JEV (MOI=0.5) for different time, followed by staining with JC-1 (10 μM). Imaging wavelength $\lambda_{ex}/\lambda_{em}$: 487/500−550 nm for green fluorescence, 560/570−620 nm for red fluorescence. Scale bars:20 μm.